Étude du comportement au cisaillement des joints actifs par émission acoustique

Zabihallah Moradian, Gérard Ballivy, Patrice Rivard, Département de Génie Civil, Université de Sherbrooke, 2500 Blv. De Université, Sherbrooke,   J1K 2R1

Résumé:
Les joints et autres discontinuités ont un rôle important dans le contrôle du comportement des structures sous conditions de charge normale et de charge cisaillement. Ils réduisent la résistance et augmentent la déformabilité de la structure. Ainsi, la gestion sécuritaire de ces structures nécessite une évaluation précise de leur stabilité en termes de résistance au cisaillement des joints de coulée dans le béton ou des autres interfaces comme les fissures planaires et la fondation sur rocher. Cette recherche porte sur l'utilisation de la méthode d'émission acoustique (EA) pour évaluer et caractériser le comportement mécanique des joints actifs. Une étude de faisabilité a été réalisée sur plusieurs échantillons de béton et de roc. Des essais de résistance au cisaillement direct sous charge normale constante (CNL) ont été réalisés dans des conditions différentes (des charges normales et des taux des déplacements diverses) et des caractéristiques différentes (rugosité variable et pourcentages de liaison diverses). Les signaux d'EA ont été acquis en utilisant des capteurs attachés aux échantillons. Deux méthodes ont été utilisées pour surveiller le comportement cisaillement de joints: 1) En utilisant la combinaison de taux des paramètres d'EA avec les graphiques de cisaillement. 2) En utilisant la combinaison des paramètres cumulés d'EA avec les graphiques de cisaillement. Quatre comportements différents des joints ont été détectés par l'EA. Ceci sera discuté en détail dans la présentation. Cette étude démontre que l'EA est utile et pertinente pour surveiller le comportement au cisaillement des joints actifs.
Mots Clés : surveillance des structures, évaluation de stabilité, joints coulées dans le béton, interfaces roc-beton, comportement au cisaillement, méthode d'émission acoustique

Monitoring shear behavior of active joints by means of acoustic emission

Abstract:
Joints and other discontinuities have an important role in controlling the behavior of the structures under normal and shear loading conditions. They reduce strength and increase deformability in structures. Thus, the safe management of these structures requires a precise evaluation of their stability in terms of the shear strength of the discontinuities such as concrete-concrete joints and concrete-rock interfaces between the structure and rock foundation. In order to evaluate the applicability of the acoustic emission (AE) as an indicator of instability of active joints in structures, an extensive feasibility study was done on several joint samples. Constant normal load direct shear tests (CNL) were conducted under different conditions (in various normal loads and displacement rates) and different joint characteristics (with various roughness and bonding percentages) and AE signals were acquired using attached sensors to the samples. AE parameters were analyzed in two different methods to monitor the shear behavior of the joints: 1) combination of the rates of the AE parameters with shear strength graph 2) combination of the cumulative AE parameters with shear strength graph. Four separated periods were observed for bonded and non-bonded joints which will be explained in the paper. In this study, acoustic emission was found to be useful and adequate for monitoring the shear behavior of the active joints.
Keywords: monitoring the structures, stability evaluation, concrete-concrete joints, rock-concrete joints, shear behavior, acoustic emission method

1. Introduction

Studying shear strength and shear behavior of joints and discontinuities in body of structures and interfaces between this body and rock foundation provides useful information about stability or instability of structures [1-4]. Previous researchers [5-11] have tried to show the mechanism of the shear stress-shear displacement graph of joints. As a summary of their works the shear behavior of the joint samples can be divided into four periods:

1. Pre-peak linear period: By applying normal and shear load on joint surface the two halves of the joint are settled and interlocked in this period. The stiffness and contact area are increased.
2. Pre-peak non-linear period: Dilatancy is generated and increased along this period because of the sliding or damaging of the secondary asperities. This period is ended by peak shear stress where steepest primary asperities are broken and dilatancy shows its maximum rate.
3. Post-peak period: All secondary and primary asperities facing the shearing direction are crushed in this period (depending on the amount of normal load) and the shear stress-shear displacement curve shows a progressive softening behavior.
4. Residual strength period: Shear stress is stable in a residual value and asperities degradation is continued in a lower severity than post-peak period.

Monitoring has acquired great importance not only for scientific community, but also for engineers and managers. Monitoring helps to understand mechanisms of disruptive processes and defining adequate prevention measures for reducing their effects. Besides conventional monitoring techniques such as extensometers, strain gages and joint meters, the AE monitoring has been experimented in several civil engineering structures [12-14]. AE is a transient elastic wave that is generated by the rapid release of energy within a material [15].

In order to apply AE for monitoring the shear behavior of in situ discontinuities, it is necessary to monitor the shear behavior of modeled joint samples in laboratory. To be specific, the system of loading can be controlled, and the reaction (emitted AE signals) of various types of joints to the loading testing conditions can be studied.

Several researches have been conducted related to the application of the AE to monitor the behavior of the geotechnical materials [16-19]. Among the most important applications of AE is its capability to monitor failure behavior, crack initiation and crack propagation of materials under loading [20-22] as well as possibility to calculate some useful parameters such as in situ stress [23].

A few researches have addressed the application of the AE for monitoring the shear behavior of the joints. Li and Nordlund [24] characterized AE during shearing of rock joints using artificial and natural joints. Their test results indicated that the AE rate peaks coincide with the stress drops caused by fracturing of asperities during joint shear [24]. Rim et al. [25] investigated the characteristics of the AE from the artificial saw tooth joints and replicas of the natural rock joints during the CNS shear test. They concluded that the shear behavior of joints can be divided into three periods according to the characteristics of AE count and AE energy [25]. They called these periods as first peak shear stress, linear increasing and second peak shear stress [25].

Hong et al. [7] performed a series of direct shear tests to investigate the influence of shear load on AE characteristics of rock-concrete interface under constant normal load. They showed that the location of the AE sources distributed over the entire shear zone before the shear stress reach converged residual value [7]. They believed that after the residual shear stress attain, the sources are localized [7]. Finally they showed that the maximum rates of count and energy were observed when the stress dropped after peak shear stress [7].

Son et al. [26] conducted laboratory shear tests under CNS and CNL conditions and studied the influence of the boundary conditions on shear behavior. From the distribution of source locations of AE it was thought that the roughness damage may be strongly correlated with roughness height [26].

In this research, laboratory direct shear test in constant normal load condition (CNL) were conducted on various kinds of joints (concrete lift joints and interface joints between concrete and rock) with different characteristics and AE and shear graphs were correlated. Two methods are proposed for monitoring the four separated periods in shear stress-shear displacement graphs of joints. The capability of the AE for predicting start point of shear stress-shear displacement graph during direct shear test is evaluated too.

2. Sample preparation and testing

Samples have been obtained from drilled cores in Manic 5 dam in Quebec, Canada. The bedrock is of very good quality from gneiss granitic rock. It is mainly composed of quartz and potassic feldspar and some biotite. The drilling was performed with a special triple tube coring system to recover intact large samples of 150mm diameters as a good representative of in situ joints. First section of a drilled core contains concrete-concrete joint (construction joint). Around the middle of the core, there is rock-concrete joint (interface between concrete and rock foundation). Final section contains rock-rock joint (rock joints in dam foundation).

The direct shear test was performed on the joint specimens in the constant normal load condition (CNL) using a direct shear apparatus mounted inside the loading frame of a rock and concrete testing machine fabricated by Materials Testing Systems (MTS).

The rate of horizontal displacement in all tests was 0.15 mm/min and the test was finished when horizontal displacement attained 10 mm. The values of shear stress and shear and normal displacements due to applied shear loads have been recorded during each test.

AEs were monitored with PAC μ-SAMOS system. This system consists of two 8-channel AE data acquisition systems (PCI-8). Four AE transducers (PAC, R3α general purpose) were used to detect AE signals. The frequency range of the sensors is 25-530 KHz, the amplification of pre-amplifier was 40 db, and AE exceeding 50 db was measured. Figure 1 shows AE system attached to MTS system.

The results of the samples number CC8.35 (non-bonded concrete-concrete joint), BCC3.45 (bonded concrete-concrete joint) and RC7.63 (non-bonded rock-concrete joint) as the typical shear behavior of all specimens are analyzed. Figures 2 and 3 show the results of direct shear test on the samples.

The laser profilometer model Kréon Zephyr 25 was used for scanning the joint surfaces. The laser emits a red, luminous plane with a wavelength of 670 nm and a maximum output power of 4 mW. The sensor has number of points/second of 30 000 and depth and width of field 90 and 25 mm. Figure 4 shows surface profilometer scanner. For measuring roughness of the joint surfaces, a 0.5 mm profile interval was chosen and the average Z2 parameter was calculated for each surface using the following equation [27].

$$Z_2 = \sqrt{\frac{1}{N}\sum_{i=1}^{N}\left(\frac{Z_{i+1} - Z_i}{\Delta Y}\right)^2}$$

Which N is the number of points on one profile; Z and Y are the coordination of the points on profiles parallel to X direction. Table 1 contains the average Z2 roughness parameter for each sample.

Table 1: Z2 parameter for each sample

No	Profile interval (mm)	Average Z2 parameter
CC8.35	0.5	0.687
RC7.63	0.5	0.487

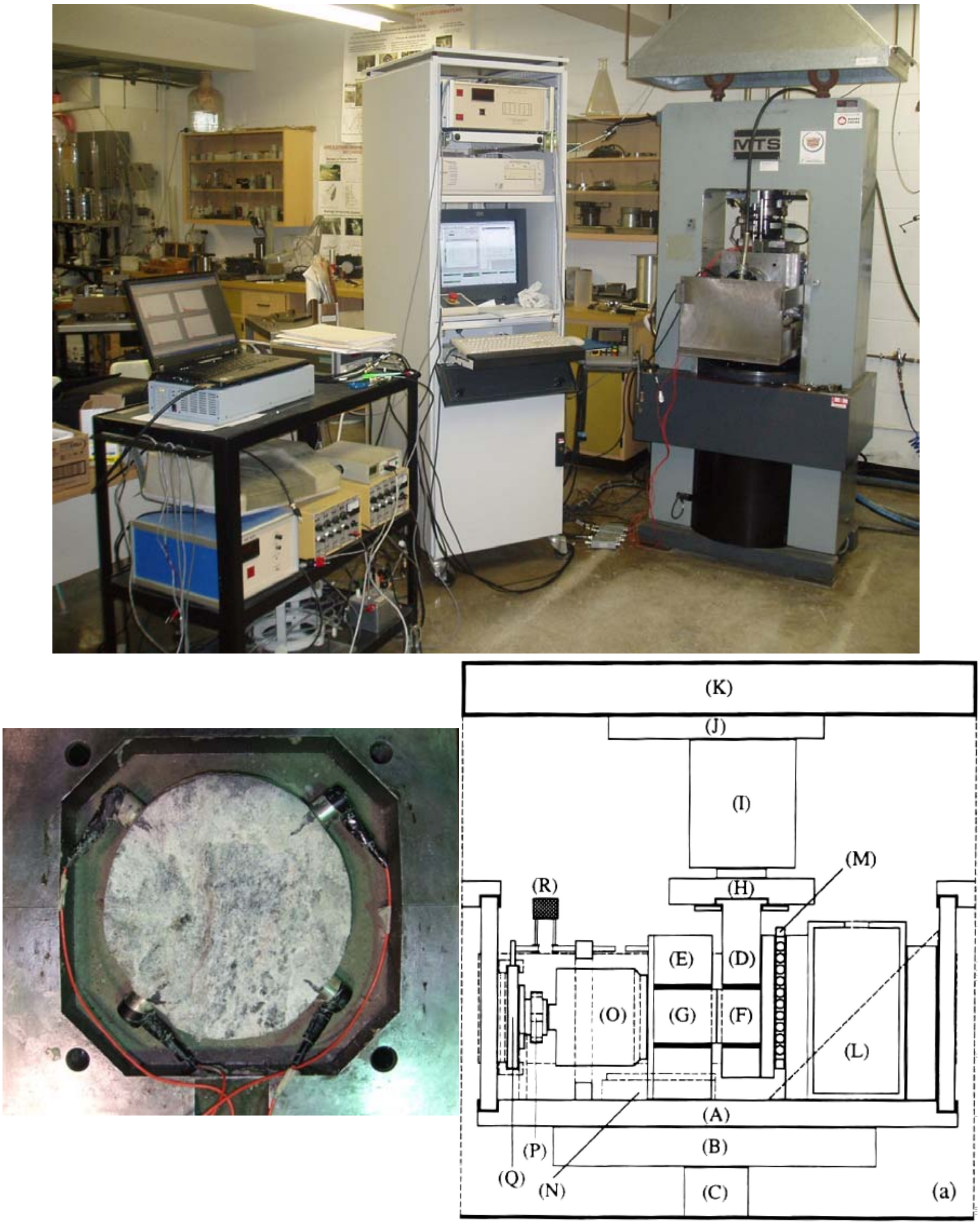

Figure 1: AE system attached to MTS system

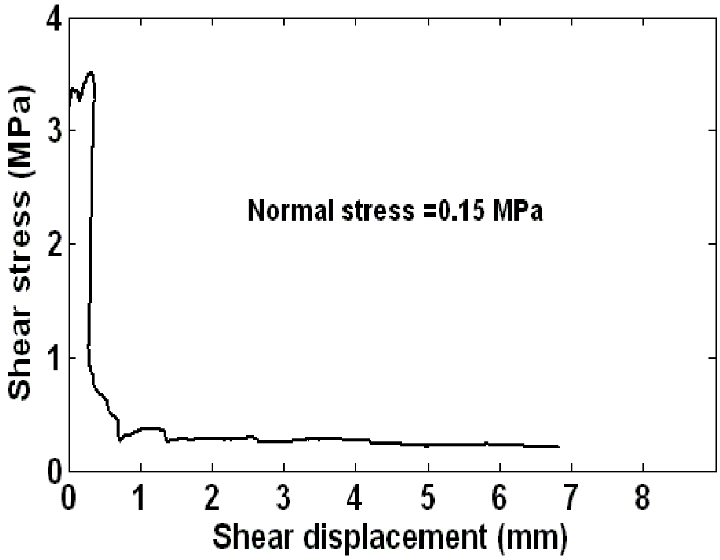

(a) Bonded concrete-concrete joint (Sample BCC3.45)

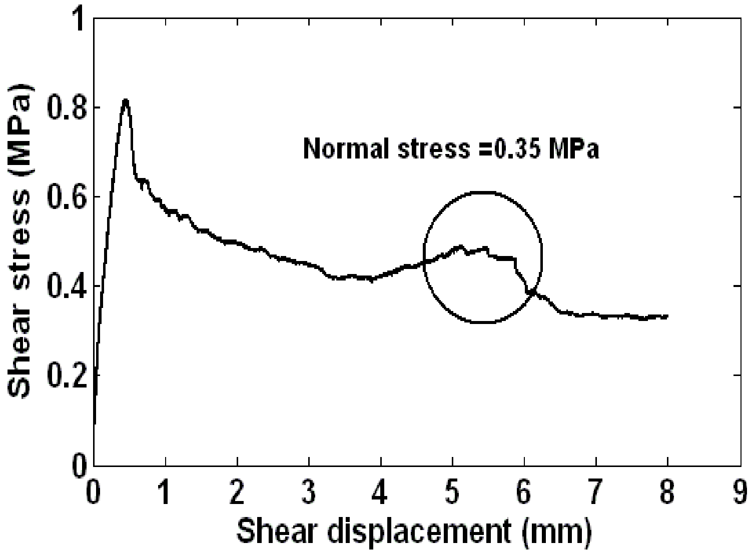

(b) Non-bonded concrete-concrete joint (Sample CC8.35)

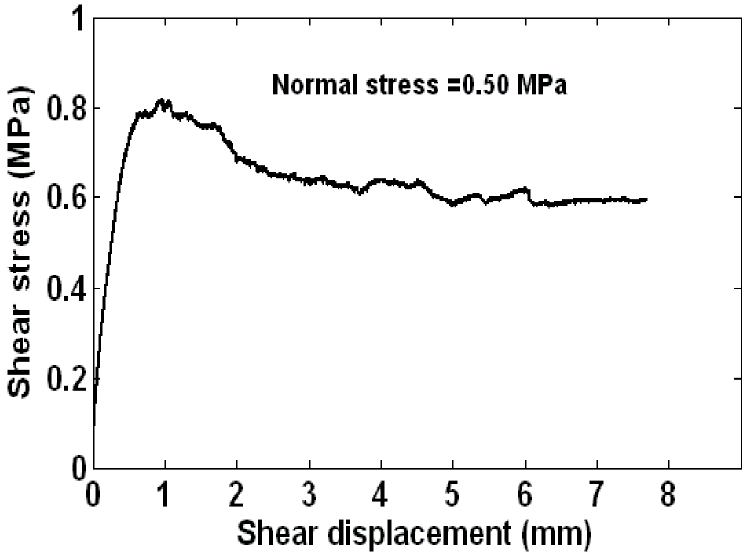

(c) Non-bonded rock-concrete joint (Sample RC7.63)

Figure 2: shear stress vs. displacement

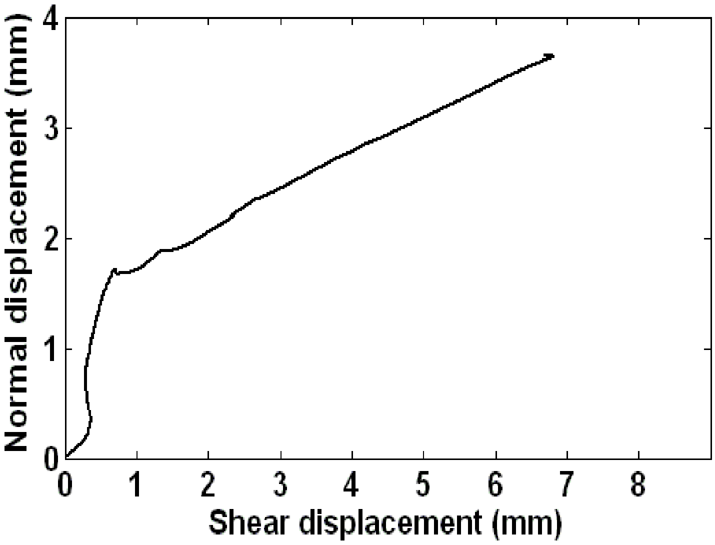

(a) Bonded concrete-concrete joint (Sample BCC3.45)

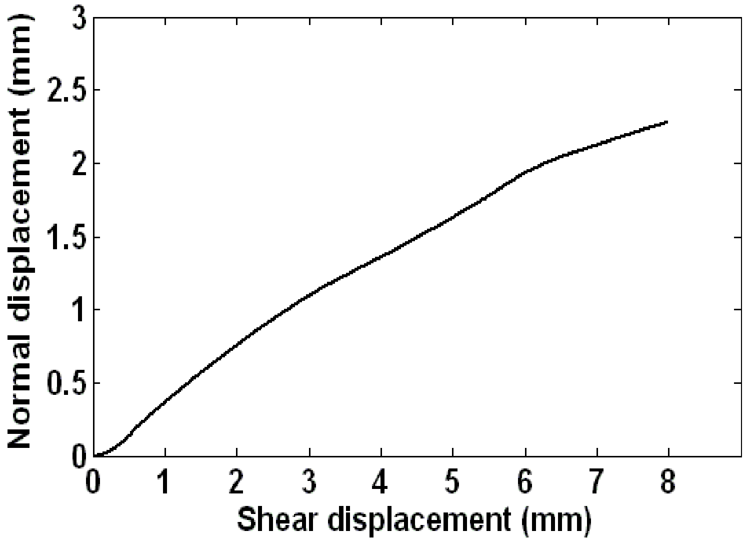

(b) Non-bonded concrete-concrete joint (Sample CC8.35)

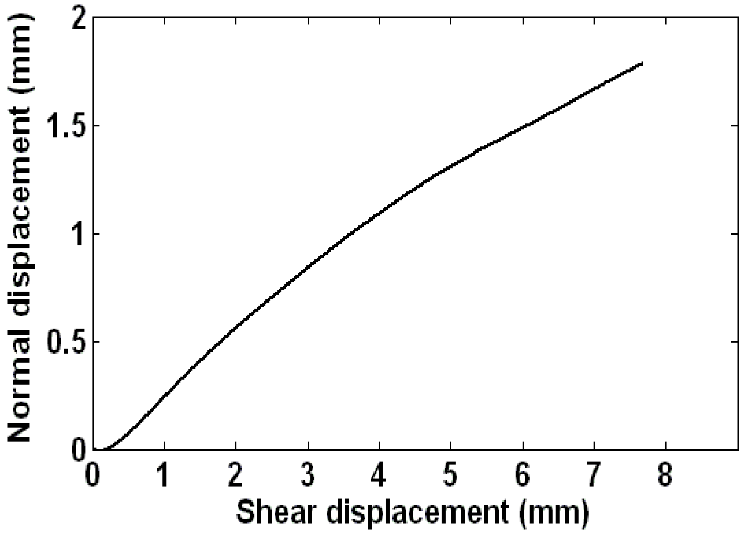

(c) Non-bonded rock-concrete joint (Sample RC7.63)

Figure 3: Normal displacement vs. shear displacement

Figure 4: surface profilometer scanner

3. Predicting the start point of the shear movement by means of AE

One of the most important issues in monitoring the behavior of the active joints is detecting point that shearing starts. When the joint starts moving, one can be aware and implement remedial solutions to inhibit the movement. By comparing the shear stress-shear displacement graphs and AE parameters graphs the start point of shear movement is shown.

Figure 2a show shear stress vs. shear displacement for bonded concrete-concrete joint (Sample BCC3.45). Although shear stress has started to increase, there is no change in shear displacement. When sample passes its elastic behavior, permanent displacements are initiated.

Figures 5a and 6a show shear stress and count and energy rate vs. time for bonded concrete-concrete joint (Sample BCC3.45) respectively. Looking at Figures 5a and 6a, it can be seen that the AE graphs have no change while there is no shear displacement. As soon as shear displacement begins, the AE parameters increase rapidly so that during failure of the sample the AE parameters attain their maximum values.

In bonded joint, by applying shear load there is no change in shear displacement and consequently in AE parameters until joint failure, but it doesn’t mean that the sample is not under loading. Using a load monitoring instrument such as load cell helps us to have a better insight about joint behavior.

The behavior of the bonded joint should be monitored by a combination of instruments because the distance between AE increasing and their maximum value (failure point) is very short and it is very difficult to predict the starting point of movement just by AE monitoring.

Figures 2b and 2c show that for non-bonded joints, shear displacement increases immediately after increasing in shear stress. The displacement generates AE signals right after the beginning of the test (Figures 5b and 5c for count rate and Figures 6b and 6c for energy rate).

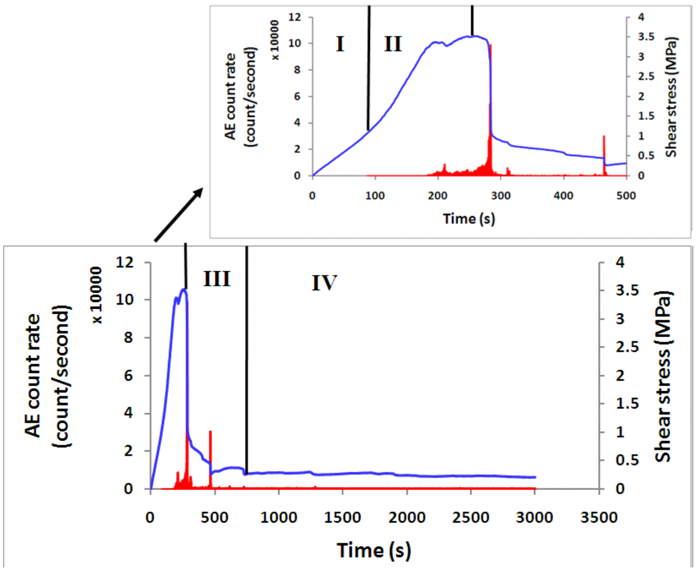

(a) Bonded concrete-concrete joint (Sample BCC3.45)

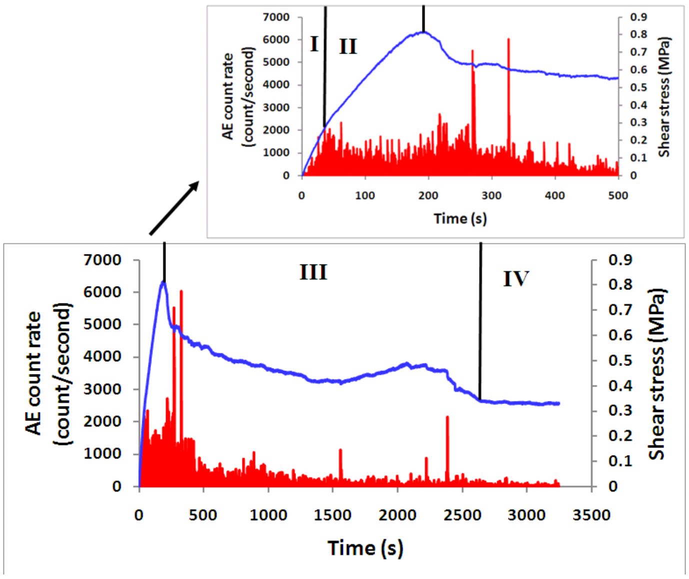

(b) Non-bonded concrete-concrete joint (Sample CC8.35)

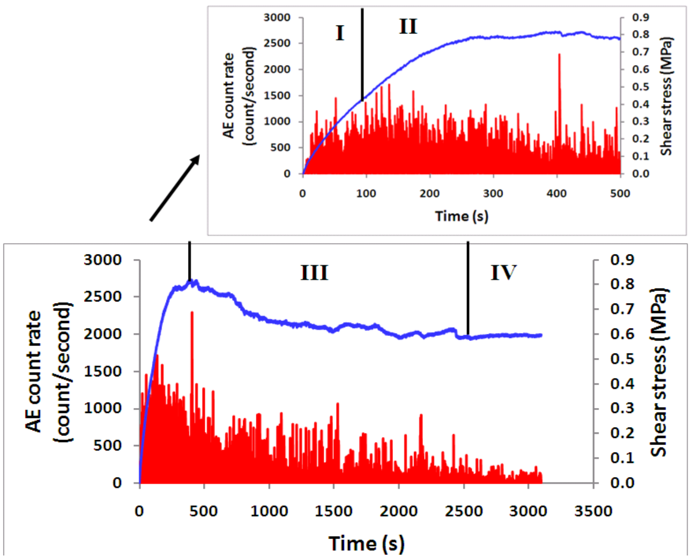

(c) Non-bonded rock-concrete joint (Sample RC7.63)

Figure 5: shear stress and AE count rate vs. time

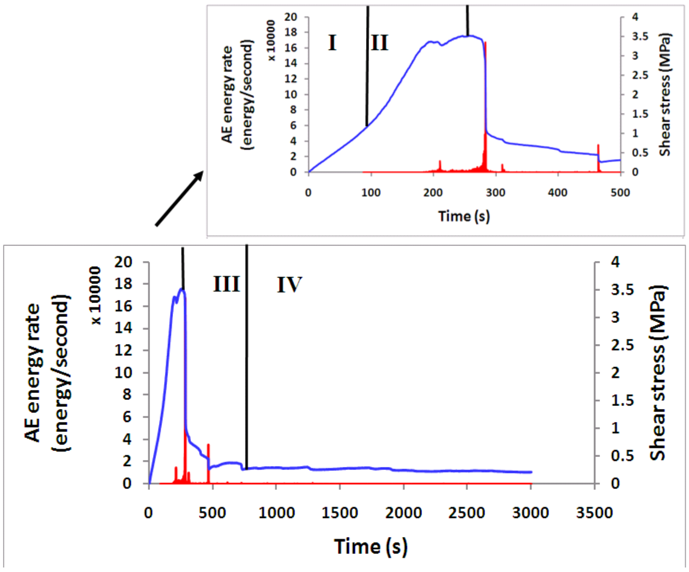

(a) Bonded concrete-concrete joint (Sample BCC3.45)

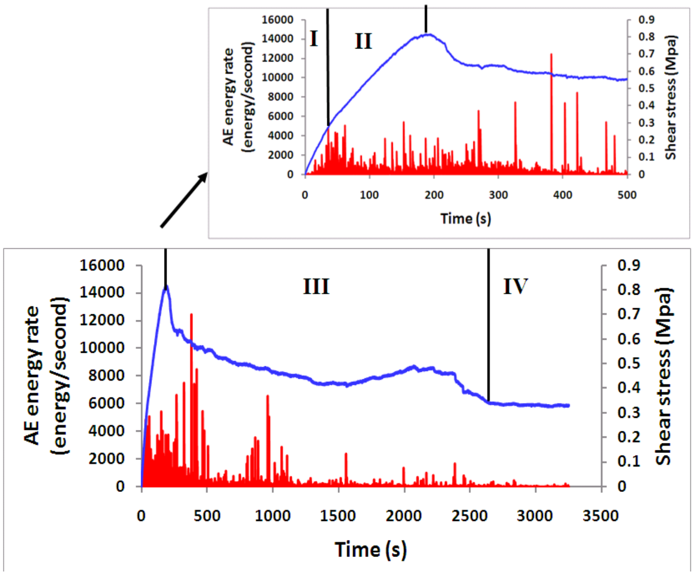

(b) Non-bonded concrete-concrete joint (Sample CC8.35)

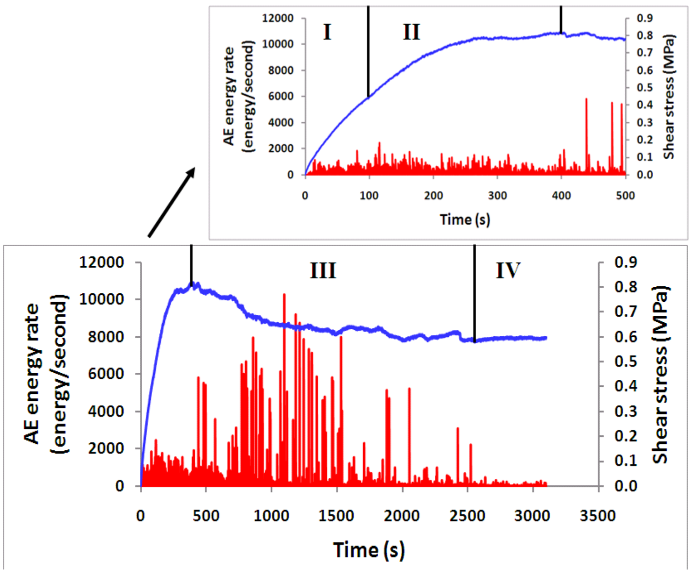

(c) Non-bonded rock-concrete joint (Sample RC7.63)

Figure 6: shear stress and AE energy rate vs. time

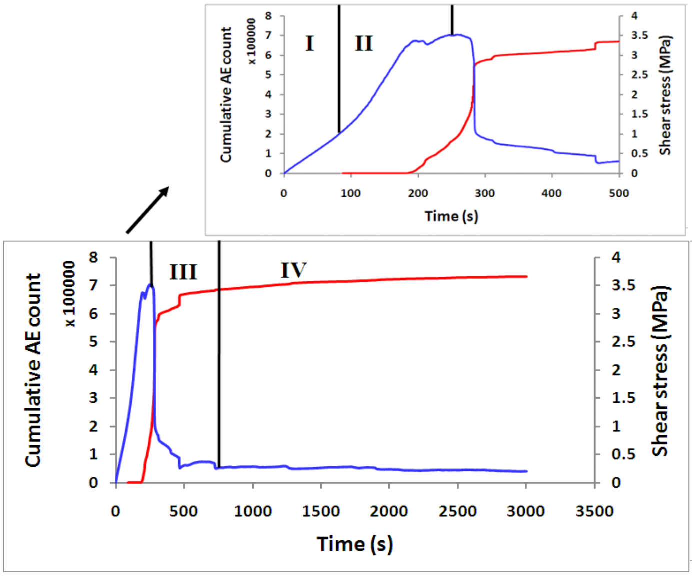

(a) Bonded concrete-concrete joint (Sample BCC3.45)

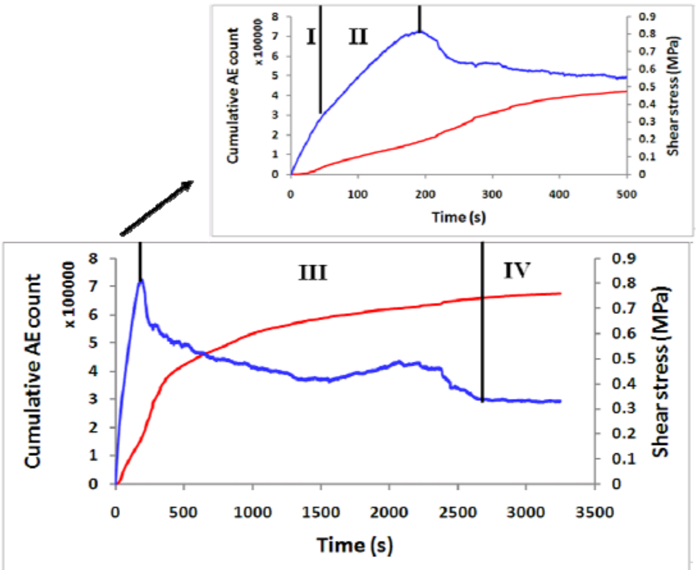

(b) Non-bonded concrete-concrete joint (Sample CC8.35)

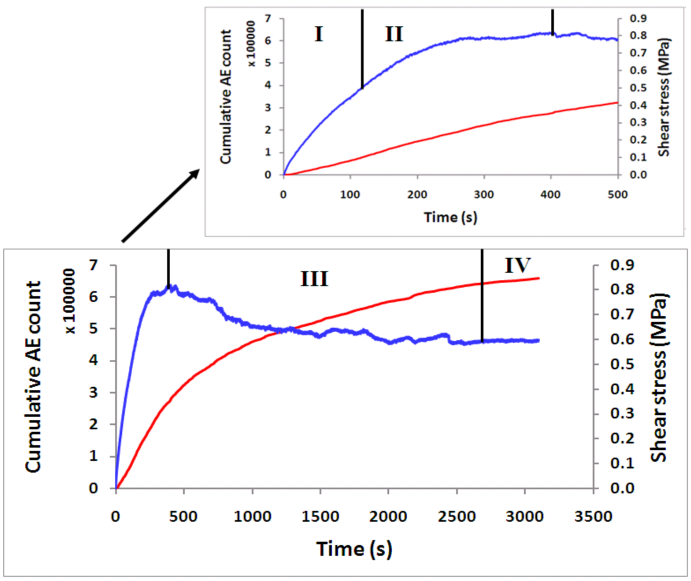

(c) Non-bonded rock-concrete joint (Sample RC7.63)

Figure 7: shear stress and cumulative AE count vs. time

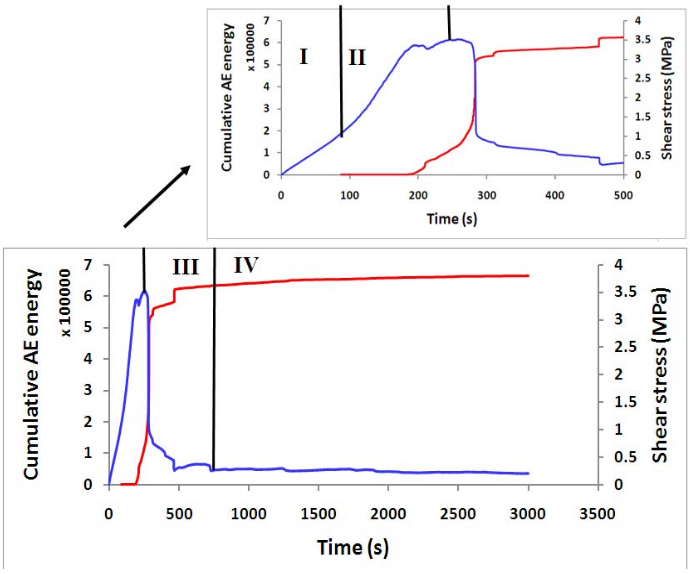

(a) Bonded concrete-concrete joint (Sample BCC3.45)

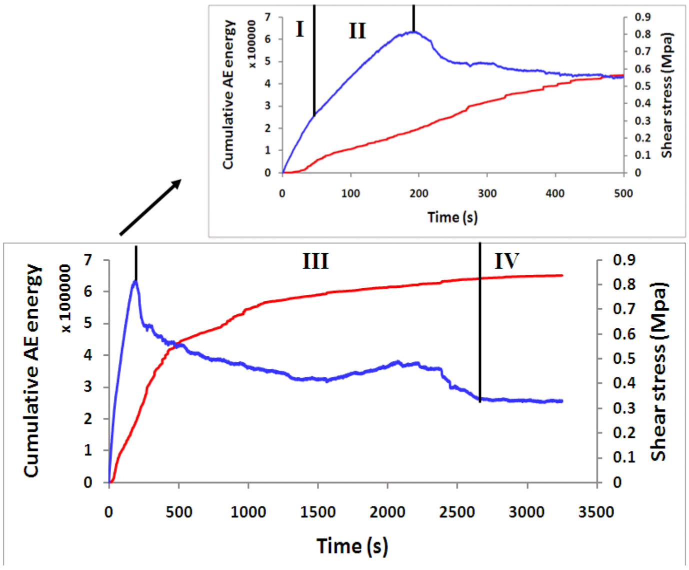

(b) Non-bonded concrete-concrete joint (Sample CC8.35)

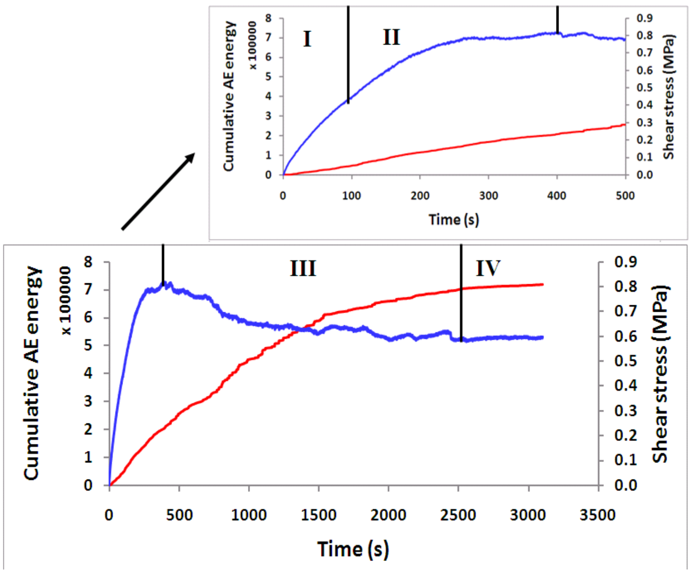

(c) Non-bonded rock-concrete joint (Sample RC7.63)

Figure 8: shear stress and cumulative AE energy vs. time

4. Monitoring pre-peak, Peak and post peak of shear strength graph by means of AE

In this section the capability of the AE for monitoring the four periods in shear stress-shear displacement graph is evaluated using the following methods.

4.1. Study on the basis of counts and energy rate

A combination of count and energy rate with shear strength vs. time has been used to correlate the shear behavior of the joints with generated AE signals (Figures 5 and 6).

For bonded joint samples (sample BCC3.45) there are no AEs in pre-peak linear period (period I). In pre-peak non-linear period (period II) some AEs are generated. They come from crack initiation and propagation in the contact surfaces. In post-peak period (period III), because of stress dropping, AEs increase dramatically and show their maximum peak. This process is due to cracking and breaking of the bonded shear surface. Following this large peak, there are some smaller peaks which are generated from damaging of the secondary and primary asperities. At the residual period of shear stress graph, count and energy rate attain their minimum values. It seems that before this period the entire primary and secondary asperities have been sheared. The only movement in this period is the sliding of the joint surfaces, so since there is no distinct shearing in this period, the count and energy rate showed low values.

Looking at non-bonded joints in Figures 5 and 6 (samples CC8.35 and RC7.63) it can be seen that in period I AEs start from background. It is believed that they come from locking of the joint halves. They show some instant peaks in this period. In period II, AEs continue increasing proportionally to loading and almost show peaks in same size before maximum shear stress. These signals are because of breaking of the secondary asperities and sliding of the primary asperities. In period III, whole asperities (secondary and primary) are sheared off. In this period AEs increase suddenly after shear stress peak, so that the maximum value of the count and energy rate is observed in this period, they decrease gradually at the end of this period. Period IV for non-bonded joints is same to bonded joints.

4.2. Study on the basis of cumulative count and energy

Figures 7 and 8 show the combination of the cumulative count and energy with shear stress graph for joint samples under study.

For bonded joint (sample BCC3.45), both cumulative count and energy graphs show nothing in pre-peak linear period. In pre-peak non-linear period they show a few signals near the end of this period. During post-peak period they show a vertically increasing and then a convexity behavior in their values and finally in residual period, they continue increasing with a very low rate.

For non-bonded joints (samples CC8.35 and RC7.63) cumulative count and energy graphs increase with concavity in pre-peak linear period and they show a linear increasing in pre-peak non-linear period. During post-peak period they show an increasing with convexity behavior. In residual period, like bonded joints, they continue increasing with a very low rate.

5. Discussion

For having a better knowledge about shear behavior of joints, 3D view and 2D profiles of the joint surfaces were drawn (Figures 9-12). Sample CC8.35 has rough surfaces with large asperities (see Figures 9 and 10, corresponding 3D view and 2D profiles for this sample). Although the joint surfaces of sample RC7.63 have a major asperity (Figure 11), it is parallel to the shear direction so that the 2D profile in this direction is almost smooth (Figure 12).

In Figure 2b, the behavior of the sample in section highlighted in circle, is just an overriding trough a major asperity. According to Figures 5b (count rate graph) and 4b (energy rate graph) there are no significant changes in this section.

Although it seems that all of primary and secondary asperities are sheared after maximum shear strength but it strongly depends on the amount of constant normal load and joint roughness, so that in low values of normal load, large asperities in samples CC8.35 with Z2=0.687 and RC7.63 with Z2=0.487 just slide on each other without any significant failure.

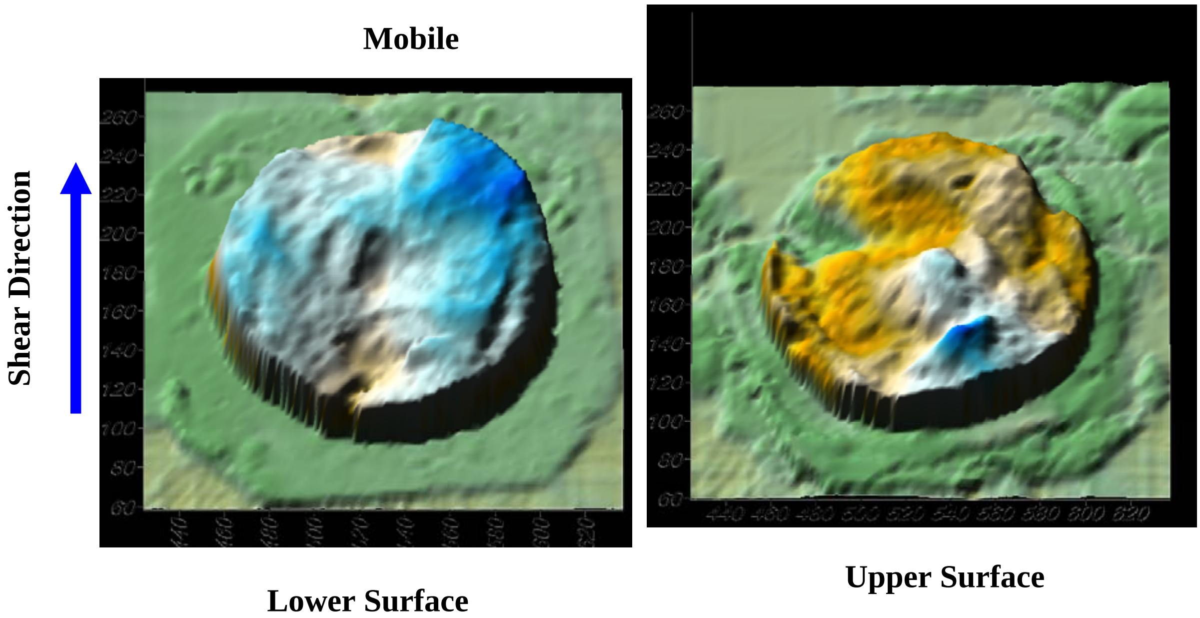

Figure 9: A 3D view of lower and upper surfaces of non- bonded Concrete-concrete joint

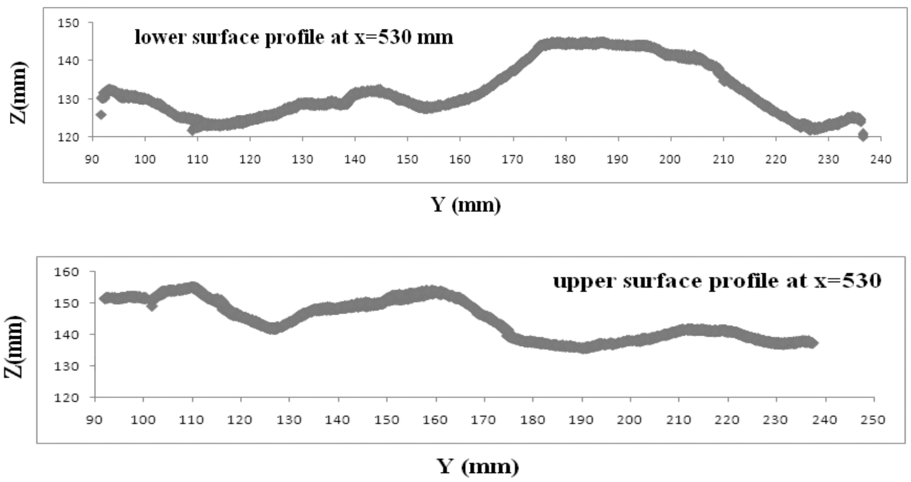

Figure 10: A profile drawn at middle of lower and upper surfaces of non-bonded Concrete-concrete joint in the direction of shearing

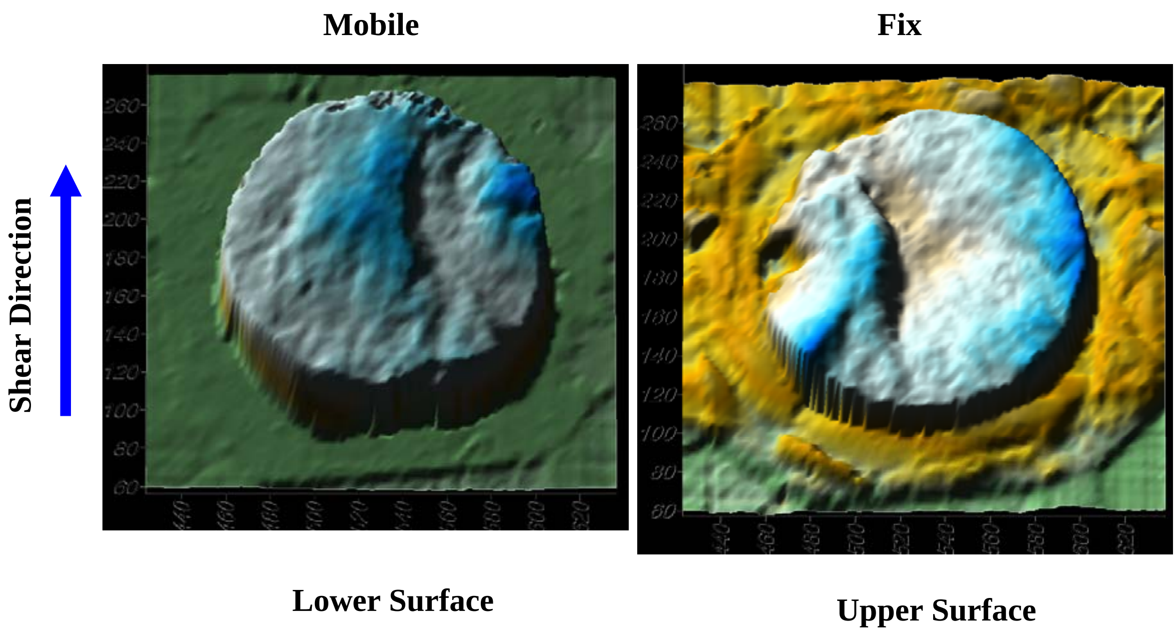

Figure 11: A 3D view of lower and upper surfaces of non-bonded Rock-concrete joint

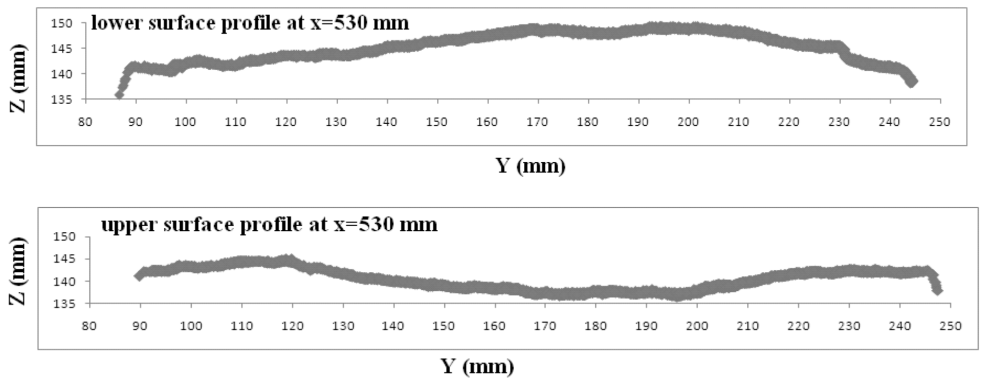

Figure 12: A profile drawn at middle of lower and upper surfaces of non-bonded Rock-concrete joint in the direction of shearing

6. Conclusions

Some direct shear tests were performed to investigate the application of the AE for monitoring the shear behavior of concrete-concrete and rock-concrete joints. AE was monitored during shearing of joints under constant normal load (CNL). Count and energy parameters were analyzed to examine the relation between shear behavior and AE.

For bonded joint, shear displacement does not start right after applying shear load; so the start point of movement cannot be detected by AE before failure. The distance between AE generation and failure is very short; therefore there is not enough time for remedial solution. A combination of other instruments such as loading measuring instruments is needed to be aware of the behavior of the joint before this point.

For non-bonded joint, shear displacement is started and AE is generated by applying shear load. In contrary to bonded joint, for these ones the distance between AE detection and failure is enough long to implement some remedial solutions.

Two methods were used to monitor pre-peak linear, pre-peak non-linear, post-peak and residual periods in shear stress-shear displacement graphs of joints: 1) Using combination of count and energy rate with shear graphs. 2) Using combination of cumulative count and energy with shear graphs. Table 2 summaries the behavior of AEs in each period using two different methods.

Table 2: Different behaviors in shear stress-shear displacement graphs monitored by AE

Periods	Behavior according to count and energy rate		Behavior according to cumulative count and energy	
	Bonded joints	**Non-bonded joints**	**Bonded joints**	**Non-bonded joints**
Pre-peak linear period	No signal	Increasing from background in low values, maybe some instant peaks	No signal	Increasing with concavity
Pre-peak non-linear period	A few signals near the end	Increasing in a constant rate with peaks in same size	Low increasing near the end	Linear Increasing
Post peak period	Increasing dramatically until maximum value and decreasing very fast	Increasing dramatically and decreasing gradually	Increasing vertically and continuing with convexity	Increasing with convexity
Residual period	Attaining minimum values with some instant peaks	Attaining minimum values with some instant peaks	increasing, with a very low rate	increasing, with a very low rate

The results of this study showed that simulating various kinds of joints and correlating AE and shear graphs in laboratory provides a better interpretation of the shear process of the in situ discontinuities when there are just the results of the AE monitoring.

7. Acknowledgement

This study was made possible by the financial assistance provided by Hydro-Quebec and NSERC grant, as well as the extensive participation of Université de Sherbrooke. The authors would like to thank Georges Lalonde, technician of the rock mechanics laboratory and Clermont Gravel for their contribution in this study.

References

[1] Lo KY, Lukajic B, Wang S, Ogawa T. Tsui KK. Evaluation of strength parameters of concrete-rock interface for dam safety assessment. Canadian dam safety conference, Toronto, September 1990: 71-93.

[2] Seidel JP, Haberfield CM. Laboratory Testing of Concrete-rock Joints in Constant Normal Stiffness Direct Shear. Geotechnical Testing Journal 2002; 25(4): 391-404.

[3] Ballivy G, Gravel C, El Malki T. Development of a new experimental protocol to estimate the shear strength of concrete-rock joints. EUROCK06 – Multiphysics Coupling and Long Term Behaviour in Rock Mechanics, Belgium 2006.

[4] Moradian ZA, Ballivy G, Gravel C, Saleh K. Analysis the Shear Strength of the active Joints Using Results of the Constant Normal Load Shear Test. 4th Asian Rock Mechanics Conference, Tehran, Iran 2008.

[5] Barton N, Choubey V. The shear strength of rock joints in theory and practice. Rock Mechanics,1977;10: 1–54.

[6] Grasselli G. Shear Strength of Rock Joints Based on Quantified Surface Description. Rock Mech. Rock Engng 2006; 39 (4): 295–314

[7] Hong C, Seokwon J. Influence of shear load on the characteristics of acoustic emission of rock-concrete interface. Key Engineering Materials 2004; 270-273:1598-1603.

[8] Kimura T, Esaki T. A new model for the shear strength of rock joints with irregular surfaces. In: Mechanics of jointed and faulted rock, HP Rossmanith, ed. Balkema, Rotterdam, 1995, pp. 133–138.

[9] Yang Z Y, Chiang D Y. An experimental study on the progressive shear behavior of rock joints with tooth-shaped asperities. Int J Rock Mech Min Sci Geomech Abstr 2000; 37(8):1247–1259.
[10] Haberfield C M, Johnston I W. A mechanistically-based model for rough rock joint. Int J Rock Mech Min Sci Geomech Abstr 1994; 31(4): 279–292.
[11] Gentier S, Riss J, Archambault G, Flamand R, Hopkins D. Influence of fracture geometry on shear behavior. Int J Rock Mech Min Sci Geomech Abstr 2000; 37(1–2): 161–174.
[12] Minemura O, Sakata N, Yuyama S, Okamoto T, Maruyama K. Acoustic emission evaluation of an arch dam during construction cooling and grouting, Construction and Building Materials 1998;12:385-392
[13] Sasao H, Hirata A, Obara Y. Measurement of acoustic emission and interpretation of its results during excavation of a rock cliff with opening joints, ISRM Technology roadmap for rock mechanics, South Africa, 2003.
[14] Shiotani T, Aggelis DG, Makishima O. Global Monitoring of Concrete Bridge Using Acoustic Emission, ICAE-6 / AEWG-50: Lake Tahoe, NV, USA, Oct 29-Nov 2, 2007.
[15] Koerner RM, McCabe WM, Lord AE. Overview of acoustic emission monitoring of rock structures, Rock Mechanics 1981;14:27-35.
[16] Falls SD, Young RP. Acoustic Emission and ultrasonic-velocity methods used to characterize the excavation disturbance associated with deep tunnels in hard rock. Techonophysics 1998;289(1–3):1–15.
[17] Maejima T, Morioka H, Mori T, Aoki K. Estimation of rock mass behavior for AE monitoring in excavation of Kannagawa underground power plant cavern. In: Proceedings of the 31st symposium on rock mechanics, 2001: 256–60.
[18] Butt SD, Muckherjee C, Lebans G. Evaluation of acoustic attenuation as an indicator of roof stability in advancing headings. Int J Rock Mech Min Sci; 2003:37:1123–31.
[19] Cai M, Kaiser PK, Morioka H, Minami M, Maejima T, Tasaka Y, Kurose H. FLAC/PFC coupled numerical simulation of AE in large-scale underground excavations. Int J Rock Mech Min Sci; 2007; 44:550-564.
[20] Eberhardt E, Stead D, Stimpson B, Read RS. Changes in acoustic event properties with progressive fracture damage, Int. J. Rock Mech. & Min. Sci; 1997;34:3–4
[21] Mlakar V, Hassani FP, Momayez M. Crack development and acoustic emission in potash rock. Int J Rock Mech Min Sci; 1993; 30:3, 305–319.
[22] Chang SH, Lee CI. Estimation of cracking and damage mechanisms in rock under triaxial compression by moment tensor analysis of acoustic emission, Int J Rock Mech Min Sci; 2004;41: 1069–1086.
[23] Seto M, Utagawa M, Katsuyama K, Nag DK, Vutukuri VS. In situ stress determination by acoustic emission technique, Int J Rock Mech &Min. Sci;1997; 34:3-4
[24] Li C, Nordlund E. Characteristics of acoustic emissions during shearing of rock joints, Rock joints, Barton & Stephanson, eds. Balkema, Rotterdam, 1990.
[25] Rim H, Hae-jun C, Bong-Ki S, Chung-In L, Jae-Joon S. Experimental study for shear behavior of pseudo rock joint under constant normal stiffness condition, Underground Space Use: Analysis of the Past and Lessons for the Future, Erdem & Solak, eds. Taylor & Francis Group, London, 2005.
[26] Son BK, Lee CI, Park YJ, Lee YK. Effect of boundary conditions on shear behaviour of rock joints around tunnel. Tunnelling and Underground Space Technology; 2006; 21:347–348.
[27] Tse R, Cruden DM. Estimating joint roughness coefficients Int J Rock Mech Min Sci; 1979;16:303-307.